Discrete Action Control for Prosthetic Digits

Agamemnon Krasoulis and Kianoush Nazarpour, *Senior Member, IEEE*

***Abstract*— We aim to develop a paradigm for simultaneous and independent control of multiple degrees of freedom (DOFs) for upper-limb prostheses. To that end, we introduce *action control*, a novel method to operate prosthetic digits with surface electromyography (EMG) based on multi-output, multi-class classification. At each time step, the decoder classifies movement intent for each controllable DOF into one of three categories: open, close, or stall (i.e., no movement). We implemented a real-time myoelectric control system using this method and evaluated it by running experiments with one unilateral and two bilateral amputees. Participants controlled a six-DOF bar interface on a computer display, with each DOF corresponding to a motor function available in multi-articulated prostheses. We show that action control can significantly and systematically outperform the state-of-the-art method of position control via multi-output regression in both task- and non-task-related measures. Using the action control paradigm, improvements in median task performance over regression-based control ranged from 20.14% to 62.32% for individual participants. Analysis of a post-experimental survey revealed that all participants rated action higher than position control in a series of qualitative questions and expressed an overall preference for the former. Action control has the potential to improve the dexterity of upper-limb prostheses. In comparison with regression-based systems, it only requires discrete instead of real-valued ground truth labels, typically collected with motion tracking systems. This feature makes the system both practical in a clinical setting and also suitable for bilateral amputation. This work is the first demonstration of myoelectric digit control in bilateral upper-limb amputees. Further investigation and pre-clinical evaluation are required to assess the translational potential of the method.**

***Index Terms*— Myoelectric control, electromyography, multi-output classification, upper-limb prosthesis.**

Manuscript received April 24, 2021; revised September 29, 2021 and February 13, 2022; accepted March 4, 2022. Date of publication March 8, 2022; date of current version March 17, 2022. This work was supported by the U.K. Engineering and Physical Sciences Research Council (EPSRC) under Grant EP/R004242/1. *(Corresponding author: Agamemnon Krasoulis.)*

This work involved human subjects in its research. Approval of all ethical and experimental procedures and protocols was granted by the Approval Body: Local Ethics Committee, Faculty of Science, Agriculture and Engineering, under Approval No. #17-NAZ-056, dated June 22, 2017.

Agamemnon Krasoulis is with the School of Engineering, Newcastle University, Newcastle upon Tyne NE1 7RU, U.K. (e-mail: agamemnon.krasoulis@newcastle.ac.uk).

Kianoush Nazarpour was with the School of Engineering, Newcastle University, Newcastle upon Tyne NE1 7RU, U.K. He is now with the School of Informatics, The University of Edinburgh, Edinburgh EH8 9AB, U.K. (e-mail: kianoush.nazarpour@ed.ac.uk).

This article has supplementary downloadable material available at https://doi.org/10.1109/TNSRE.2022.3157710, provided by the authors.

Digital Object Identifier 10.1109/TNSRE.2022.3157710

I. Introduction

MODERN hand prostheses offer the potential of partially restoring the functionality of a missing upper-limb. They are typically controlled by muscular activity signals recorded on the skin surface using electromyography (EMG) signals. Nowadays, there exist commercial systems allowing for grip selection and activation based on machine learning algorithms. Nevertheless, from a technical perspective the holy grail of upper-limb prosthetics research is the simultaneous and independent control of multiple degrees of freedom (DOFs), including wrist and digit artificial joints [1]. This currently seems as the only way to approximate the remarkable dexterity of the human hand, which is still considered as the nature's most versatile end-effector [2].

Significant efforts have been made towards achieving simultaneous, multi-DOF myoelectric control. The term *proportional control* is often used to describe the feasibility of controlling one or more prosthesis output(s) in a continuous space [3]. To that end, many research groups, including us, have used multi-output regression-based algorithms to map features extracted from surface or intramuscular EMG channels onto wrist [4]–[8] and/or finger position [9]–[15], velocity [16], and force trajectories [17]–[20]. For prosthetic digit control, several studies have shown promise in decoding position/velocity offline [9], [11]–[13], [15], [16], however, only a smaller number have achieved real-time digit control in amputees [10], [14], [21]. This indicates that, to date, reconstruction of position/velocity trajectories from surface EMG signals in real-time remains a challenging problem.

In this work, we introduce *action control*, a novel paradigm for simultaneous and independent control of multiple prosthetic digits. Our approach simplifies the movement intent decoding component and makes the system more practical. In the heart of the algorithm lies a multi-output, multi-class classifier, which decodes movement intent for each controllable DOF into one of three classes (i.e., *actions*): open, close, or stall (i.e., no movement). A schematic diagram of this concept is shown in Fig. 1. From a control theory point of view, action control can be viewed as an extreme, discretized case of velocity control. The relationship between digit positions, velocities and actions is illustrated in Fig. 2. Despite using a classifier, action control allows digit positions to take values within a large set that is defined by the action step (i.e., position increase/decrease resolution). That is, by selecting a relatively small step, digit movement essentially becomes continuous. One practical advantage of this method over regression-based position control is that

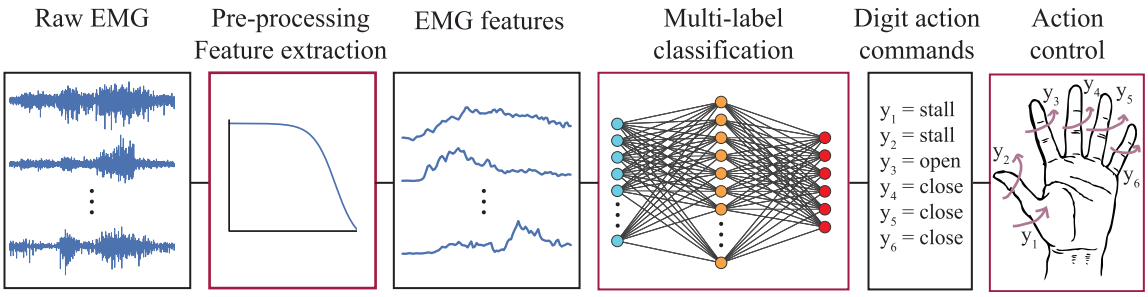

Fig. 1. Action control concept. At each time step, raw EMG signals are pre-processed and fed to a multi-output classifier with six discrete outputs. These can take one of three possible values (i.e., *actions*): open, close or stall (i.e., no movement). Each output controls one DOF of a multi-articulated prosthesis: thumb opposition/reposition, thumb abduction/adduction, and flexion/extension of the index, middle, ring, and little digits.

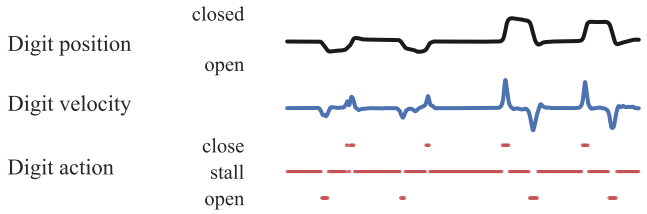

Fig. 2. Relationship between digit position, velocity and action. Action control can be viewed as a discretized version of velocity control. Note that digit positions/velocities are not required for action control. Digit positions (top row) were collected from an able-bodied subject using a CyberGlove Systems® CyberGlove II data glove. Digit velocities (middle row) are computed from digit positions using first-order differentiation. Digit actions (bottom row) are computed from digit velocities using thresholding.

it allows for collection of noise-free ground truth labels, without relying upon the use of motion tracking hardware (e.g., data gloves).

In a proof-of-concept study, we have previously demonstrated that users can employ the action control scheme to achieve comparable performance to joint angle (i.e. position) control in a robotic hand tele-operation task with an instrumented data glove [22]. In addition, we have performed a systematic offline investigation of multi-output classification for digit action decoding [23]. Here, we provide for the first time a real-time implementation of the algorithm for myoelectric digit control. We test the performance of our approach with one unilateral and two bilateral amputees and benchmark it against the state-of-the-art in myoelectric digit control, that is, regression-based joint position control. We discuss the advantages of our method over the regression-based approach and propose ideas for further improvement and pre-clinical evaluation.

II. Methods

A. Participant Recruitment

Three transradial (i.e., below-elbow) amputee volunteer participants were recruited (two female, one male; median age 59). Participants 1 and 2 were bilateral amputees and participant 3 was unilateral. Paritcipant 1 performed the experiment using their right side. Participant 2 took part in two sessions on the same day using alternate sides (i.e., right one in the morning session and left one in the afternoon session). Depending on the side used in each session, the participant is referred to as 2R or 2L (right or left side, respectively).

TABLE I
Participant Demographic Information

P	S	A	AT	AS	AC	YSA	FL	FC
1	F	67	Tran.	Bilat.	Sepsis	5	13	22
2R	F	42	Tran.	Bilat.	Sepsis	6.5	15	20.5
2L							15	20.5
3	M	59	Tran.	Right	Epithelioid sarcoma	18	17	27

Abbreviations: P, participant; S, sex (biological); A, age; AT, amputation type; AS, amputated side; AC, amputation cause; YSA, years since amputation; FL, forearm length (cm); FC, forearm circumference (cm); Tran., transradial; Bilat., bilateral.

All participants had normal or corrected to normal vision and reported being able to discriminate red from blue (i.e., no color blindness). All three subjects had previously participated in laboratory myoelectric control experiments [24]–[26], but none of them use myoelectric control in their everyday lives. Detailed demographic information about the participants is provided in Table I.

All experimental procedures were in accordance with the Declaration of Helsinki and approved by the local ethics committee. All participants read an information sheet and gave written informed consent prior to the experimental sessions.

B. Apparatus

The apparatus used in the study comprised a surface EMG recording system and a state-of-the-art, multi-articulated prosthetic hand.

1) Surface EMG Recording System: We recorded myoelectric signals using a Delsys® Trigno™ wireless system. We used 16 EMG sensors, which included 12 standard Trigno and four Trigno Mini sensors. Prior to electrode placement, we cleansed participants' skin using 70% isopropyl alcohol swabs. We then placed the EMG sensors in two rows of eight equidistant electrodes below the elbow without targeting specific muscles. In each row, we placed six standard and two mini sensors. We attached the transmitter units for the mini sensors on the participants' skin above the elbow as shown in Fig. 3(a). Upon visual inspection of the signal quality of all EMG channels, we secured the electrode positions using adhesive elastic bandage. For data acquisition, we used proprietary software provided by the manufacturer. The sampling rate for all channels was fixed at 2 kHz.

2) Prosthetic Hand: We used the multi-articulated Össur® Robo-limb hand to demonstrate target postures to participants.

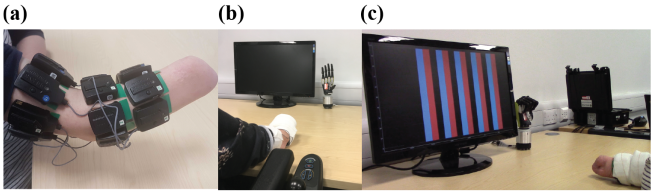

Fig. 3. Experimental protocol. (a) Electrode placement for one subject. Sixteen surface EMG electrodes were placed below the elbow arranged in two rows of eight electrodes. A combination of classic Delsys Trigno and Trigno Mini electrodes were used. The transmitter components for the mini sensors were placed above the elbow. (b) Training data collection. Participants performed imaginary movements of single-digit and full-hand grips that were instructed on the prosthesis. (c) Real-time decoding. Participants controlled the position of six bars on a screen. Target postures were instructed on the prosthesis prior to the start of the trial. The target posture in the shown trial was the "lateral" grip.

This model, which is almost identical to the commercial i-Limb^{TM} Ultra Revolution prosthesis, comprises six motors controlling the following DOFs: thumb opposition/reposition, thumb abduction/adduction, and index, middle, ring and little finger flexion/extension. Throughout the experiments, the hand was placed on a desktop base and powered via an external power supply unit (7.4 V, 7 A). The hand was controlled by a laptop computer using a CAN bus connection (baud rate: 1 MHz). We used a right-hand model for participants 1, 2R and 3 and a left-hand model for participant 2L.

C. Experimental Paradigm

Following EMG sensor placement, participants sat comfortably on an office chair and rested their arm on a table. Experimental sessions comprised two phases: *training data collection* and *real-time myoelectric control*. The two sessions were interleaved with a 10-minute break, during which participants were allowed to move freely in the lab space.

1) Training Data Collection: In the first part of the experiment, participants performed a series of imaginary finger movements that were instructed to them on the prosthesis, while surface EMG data were recorded from their upper-limb (Fig. 3). We included a combination of single-finger and full-hand grip patterns: thumb opposition/reposition; thumb abduction/adduction, and index, middle, ring and little finger flexion/extension; cylindrical and lateral grip opening/closing; and rest (i.e., no movement). We instructed participants to perform the exercises smoothly and track the prosthesis movement as closely as possible.

For each exercise, the opening/closing, opposition/reposition to flexion/extension parts were separate. Thus, the total number of exercises, including rest, was 17. Each exercise was repeated 12 times and each repetition lasted 1.3 s, which was the time required for the prosthesis to complete the demonstration at a moderate speed. Participants were given 2 s of rest in-between consecutive trials. The total duration of training data collection was approximately 12 minutes.

2) Real-Time Myoelectric Control: In the second part of the experiment, participants were instructed to use their muscles to control a six-dimensional bar interface as shown in Fig. 3(c).

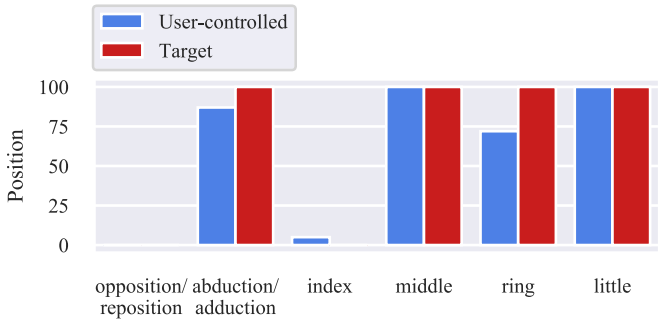

Fig. 4. Real-time control task. Participants used their muscles to control the position of six bars on the screen, each corresponding to one DOF (from left to right: thumb opposition/reposition, thumb abduction/adduction, and index, middle, ring, and little finger flexion/extension). For each DOF, blue and red bars indicate the user-controlled and target positions, respectively. The shown example corresponds to the index pointer with the following target positions: thumb fully adducted, middle, ring, and little digits fully flexed (i.e., target bars 2, 4, 5 and 6 in maximum position), thumb fully reposed, and index finger fully extended (i.e., target bars 1 and 3 in minimum position).

Visual feedback was continuously provided at an update rate of 15.625 Hz (Section II-D) on a 17" LCD flat panel display positioned 1 m in front of the participants.

An illustration of the experimental task is given in Fig. 4. Each pair of bars corresponded to one of the following DOFs: thumb opposition/reposition and thumb, index, middle, ring, and little finger flexion/extension. The blue bars were controlled by the participants and showed *actual* positions of the six DOFs. The red bars were kept fixed within the trial and corresponded to *target* positions. Participants were instructed to match the blue to red bars as closely as possible.

The following target movements were included: full thumb reposition; full flexion of the thumb, index, middle, ring, and little fingers; cylindrical, lateral, and tripod grips; and index pointer. Participants performed 10 blocks of trials for each of two control conditions (Section II-E), that is, a total of 20 blocks. Every target posture was included exactly once within a single block in a pseudo-randomized order.

Prior to the start of a trial, the target posture was demonstrated on the prosthesis. During pilot experiments we observed that, due to the dimensionality of the output space (i.e., six DOFs), demonstrating the target postures to participants ahead of the trial start was crucial for them to quickly and unambiguously perceive the exact target posture. Once the demonstration was complete, an audio cue (sine wave; frequency 1000 Hz; duration 200 ms) initiated the start of the *preparation phase* of the trial and the bar interface appeared on the display (Fig. 4). Participants were then given 5 s to match the controlled posture (i.e., blue bars) to the target (i.e., red bars) as closely as possible. At the end of this period, a second cue indicated the start of the *evaluation phase* of the trial, which lasted for 1 s. During the evaluation phase, participants were instructed to retain the output state. At the end of the trial, the bar interface disappeared from the display and participants received a score characterizing their performance during the evaluation phase (Section II-G).

The prosthesis was also reset to the neutral (i.e., resting) posture. Consecutive trials were interleaved with 2.5 s of rest.

D. Signal Pre-Processing

Data were acquired and processed every 64 ms, which translates into 128 new samples/channel at a 2 kHz sampling rate. The data processing and display update rate was thus $1/0.064$ s $= 15.625$ Hz. We processed EMG signals using a 128 ms sliding window (i.e., 50% overlap). We extracted two EMG features from each channel, namely, waveform length and log-variance [5]. We based our selection on previous findings showing that these features are effective both for multi-output regression and classification [14], [23]. We used the same EMG processing pipeline for the two control schemes presented in the following section.

E. Control Schemes and Decoder Training

We implemented the *action control* method and compared it with the state-of-the-art approach of *position control*. The two algorithms are based on multi-output classification and regression, respectively.

All models were trained during the interval between the data collection and real-time control parts using subject-specific data. During pilot experiments with able-bodied participants, we observed that individuals required a couple of trials to familiarize themselves with a new exercise and perform the demonstrated movement with their hand. Based on this observation, we discarded the first two repetitions for each exercise and, thus, the final number of repetitions per training exercise was 10. We followed this procedure to avoid label mismatches (i.e., label noise) in the training data sets. This type of label noise mostly originated from a latency between the demonstrated and performed movements, whenever a new exercise was introduced to a participant.

Throughout the experimental sessions, participants were blind to the control scheme being used. Furthermore, they were given no specific instructions on how to activate their muscles. This applied to both the preparation and evaluation phases of the trials. That is, participants were not specifically instructed whether to retain or relax their muscle activity once they had reached a desired target posture.

1) Action Control: With action control, participants controlled the bar heights on the display by taking at each time step discrete actions in order to reach the desired positions. With this control mode, the EMG features were mapped onto a discrete six-dimensional vector using multi-output classification as shown in Fig. 1. Each element in the output vector corresponded to one of the six available DOFs and could take one of three values: open, close or stall (i.e., no movement). We set the action step for the "open" and "close" commands such that a single-DOF movement from the bottom to top position, or vice-versa, would require 1.5 s. This translated in using an action step of 0.043. Based on previous findings [23], we trained six independent linear discriminant analysis (LDA) classifiers, one for each available DOF.

We post-processed predictions using a confidence rejection strategy based on false positive rate minimisation [26], [27]. Class-specific thresholds were identified for each output using training data and 10-fold cross-validation, such that the false positive rate did not exceed a global cutoff threshold (set a priori to $\theta_c = 0.2$). During inference (i.e., real-time control), predictions that were made with posterior probabilities smaller than the class-specific thresholds were discarded by the controller. Let us illustrate this with an example. Assume that for the j^{th} DOF the rejection threshold for the "open" class is $\theta^j_{open} = 0.98$. Also assume that at time step t, this DOF is stalled. If at step $t+1$ the prediction for the same DOF is "open", and the associated posterior probability is $p = 0.9$, then the controller will discard the new prediction and the DOF will hold its previous state, that is, it will remain stalled. For a more detailed description of this confidence-based rejection strategy, we refer the reader to our previous work [26].

2) Position Control: With position control, participants directly controlled the bar heights on the display. That is, the digit position trajectories were reconstructed from EMG features using multi-output linear regression, as follows:

$$\boldsymbol{y} = W^T \boldsymbol{x}, \tag{1}$$

where $\boldsymbol{x} \in \mathcal{R}^d$ is the EMG feature vector, $\boldsymbol{y} \in \mathcal{R}^m$ is the vector of estimated digit positions, and $W \in \mathcal{R}^{d \times m}$ is a weight matrix mapping input EMG features onto digit positions. The input and output dimensionalities are $d = 32$ and $m = 6$, respectively. The output vector was normalized between 0 (i.e., digit fully extended or thumb fully adducted/reposed) and 1 (i.e., digit fully flexed or thumb fully abducted/opposed). Following previous work on wrist and digit position decoding [10], [14], [28], [29], predictions were low-pass filtered in the time-domain using single exponential smoothing as follows:

$$\tilde{y}_j[n] = \alpha \cdot y_j[n] + (1-\alpha) \cdot \tilde{y}_j[n-1], \tag{2}$$

where $y_j[n]$ and $\tilde{y}_j[n]$ denote, respectively, the raw and smoothed predictions of the j^{th} DOF at time step n, and α is the smoothing parameter, set a priori to $a = 0.05$ [14].

F. Training Data Labelling

To train myoelectric decoders, ground truth data are required for both regression and classification tasks. In the former case, ground truth labels are real-valued, whereas in the latter they are discrete. In our experiments, labels were acquired using the prosthesis demonstrations presented to participants during the data collection phase.

For training regression models (i.e., position control), for which real-valued ground truth labels are required, we adopted the following strategy: at the start and end of each trial, each of the six DOFs are in one of the two extreme positions (i.e., thumb fully opposed/reposed and abducted/adducted, and all other digits fully flexed/extended). Hence, the ground truth starting and ending points are known. Within the trial, the positions of those DOFs that are involved in the specific exercise are linearly interpolated between the respective starting and ending points. On the other hand, ground truth positions for those DOFs that are not involved in the trial movement are kept fixed and equal to their starting positions. To illustrate

this approach, consider as an example the thumb opposition exercise. Assume $\boldsymbol{y} \in \mathbb{R}^6$ denotes the position vector with the first element corresponding to thumb opposition, the second element corresponding to thumb abduction, the third element corresponding to index flexion and so on. At the start of the trial, all digits are fully extended and the thumb is fully adducted and reposed. Thus, the ground truth starting point is $\boldsymbol{y} = [0, 0, 0, 0, 0, 0]^\top$. At the end of the trial, only the thumb has moved to the fully opposed position. That is, the ground truth ending point is $\boldsymbol{y} = [1, 0, 0, 0, 0, 0]^\top$. The position of the thumb opposition DOF is linearly interpolated within the trial, which lasts for 1.3 s. Note that this is exactly the time it takes for the prosthesis to demonstrate the exercise. For instance, at $t = 0.65$ s, the ground truth position is approximated as $\boldsymbol{y} = [0.5, 0, 0, 0, 0, 0]^\top$.

Data labelling for multi-output classification models (i.e., action control) is simpler, since in this case ground truth labels are discrete. That is, $\boldsymbol{y} \in \mathbb{S}^6$, where $\mathbb{S} = \{\text{open, stall, close}\}$ and we assume the same ordering in $\boldsymbol{y}$ as in the regression example above. For classification, however, we only need to know which DOFs are moving within a trial and in which direction. Considering again the thumb opposition example as above, the ground truth vector for the whole duration of the trial is $\boldsymbol{y} = [\text{close, stall, stall, stall, stall, stall}]^\top$, where "close" in the case of the thumb opposition DOF indicates opposition.

G. Performance Evaluation

At the end of each trial, participants received a score on the screen characterizing their performance during the evaluation phase of the trial. The score ranged from 0% to 100% and was based on the multivariate median absolute error MAE_{mv} between the target and performed postures:

$$MAE_{mv} = \frac{1}{D}\sum_{j=1}^{D} Mdn|\boldsymbol{y}^j - \hat{\boldsymbol{y}}^j|, \tag{3}$$

where $\boldsymbol{y}^j \in \mathbb{R}^N$ and $\hat{\boldsymbol{y}}^j \in \mathbb{R}^N$ denote the vectors containing the target and performed position trajectories during the evaluation phase for the j^{th} DOF, $N = 16$ is the number of display updates (i.e., time steps) in the evaluation phase, $D = 6$ is the number of controllable DOFs, and Mdn denotes the median operator. The target position trajectories $\boldsymbol{y}^j$ are known and constant (i.e., equal to the heights of the red bars in Fig. 4). On the other hand, the controlled position trajectories $\hat{\boldsymbol{y}}^j$ (i.e., the heights of blue bars) are variable, as they are controlled by the participant.

We transformed MAE_{mv} into an intuitive for the user performance score with the following principles in mind: 1) the score range should be from 0% to 100%; 2) a perfect match between the target and performed postures should result in a 100% score; and 3) a very poor or random prediction, defined as $MAE_{mv} > 0.5$, should yield a 0% score. Taking the above into consideration, we implemented this transformation as follows:

$$score = 2 \times \max\{0.5 - MAE_{mv}, 0\} \times 100\,(\%)\,. \tag{4}$$

To assess offline decoding performance on the training set, we used 10-fold cross-validation. Within each iteration, nine out of 10 repetitions from all exercises were used for training and the remaining repetition was used for testing. We report the average performance across folds. For multi-output regression we use the multivariate (R^2) score and for multi-output classification we report macro-average—both across outputs and class labels— F1-score (i.e., harmonic mean of precision and recall).

H. Non-Tasked-Related Measures

In addition to control performance, we assessed the two control schemes in terms of two non-task-related measures: *muscle contraction intensity* and *output stability*. For the former, we computed the raw EMG power across all channels during whole trial duration. For the latter, we estimated average output variability (i.e., standard deviation) during the trial evaluation phase.

I. Post-Experimental Questionnaire

At the end of each experimental session, participants were asked to respond to a short questionnaire. Concretely, they were asked to rate the two control schemes (i.e., action and position control) on a scale from 1 (strongly disagree) to 5 (strongly agree), based on the following statements:

1) the control interface was easy;
2) the control interface was intuitive;
3) I found it easy to adapt to the control interface.

Half scores, for example 3.5, were allowed. Participants were also asked to indicate their overall preference. Participant 2 responded to the questionnaire twice, once after each session, and the respective scores were averaged.

J. Implementation

The experiment was implemented in `Python` (v3.7) and all sessions were run on a standard laptop computer (16 GB, i7 2.70 GHz). Data collection, processing, and the real-time myoelectric control interface were implemented using the `axopy` library (v0.2.3) [30] and custom-written code. Model training and inference were performed using the `scikit-learn` library (v0.22) [31].

K. Statistical Analysis

Due to the small number of participants, we adopted the *small-N* experimental design and performed independent statistical analyses at the participant/session level [8]. We used two-sided Wilcoxon (i.e., non-parametric) tests to perform comparisons between action and position control and employed the Holm-Bonferroni correction to account for multiple comparisons (i.e., four). The target presentation order was identical for the two conditions and, hence, all measurements were paired. The condition order was counterbalanced: participants 1 and 2L first performed the task with action and then position control, and participants 2R and 3 with the reversed order. We performed all statistical analyses in `Python` (v3.7) using the `Pingouin` library (v0.3.1) [32].

TABLE II
OFFLINE PERFORMANCE

Participant	R^2	F1-score
1	0.51	0.82
2R	0.38	0.74
2L	0.40	0.78
3	0.51	0.82

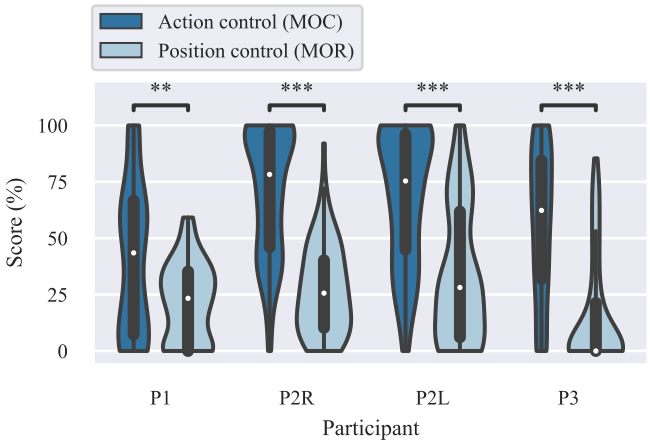

Fig. 5. Performance comparison for action (i.e., multi-output classification) and position (i.e., multi-output regression) control. Higher scores are better. Points, medians; solid boxes, interquartile ranges; whiskers, overall ranges of data; violins, kernel density estimates of underlying data distributions; double asterisk, $p < 0.01$; triple asterisk, $p < 0.001$; MOR, multi-output regression; MOC, multi-output classification.

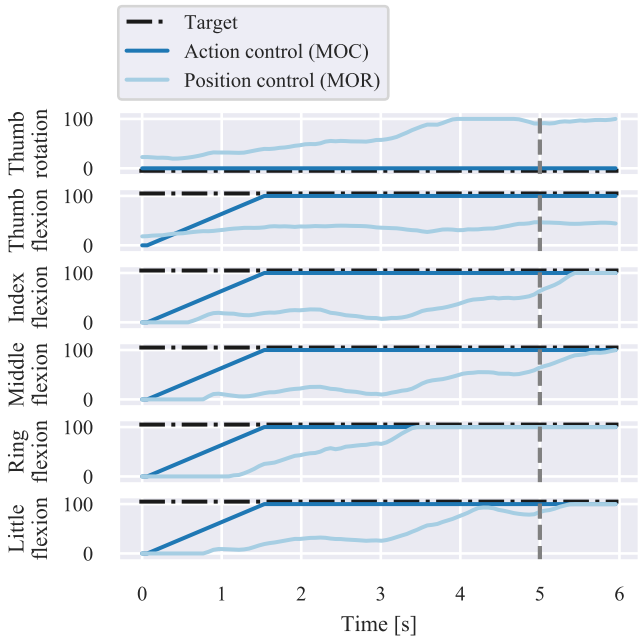

Fig. 6. Representative trial. The positions of the six DOFs are juxtaposed for action and position control within the course of one trial. The shown example corresponds to participant 2R and the "lateral grip", with the following target positions (black dashed lines): full thumb reposition and adduction, and full flexion of all digits. Vertical grey lines indicate the start of the evaluation phase of the trial. Performance scores for the shown trial were 100% and 46.44% with action and position control, respectively. A small offset has been added to target positions for illustration purposes.

III. RESULTS

A. Offline Training and Analysis

The results of the offline analysis performed as part of model training are presented in Table II. The median macro-average F1-score for multi-output classification (i.e., action control) was 0.80 (ranging from 0.74 to 0.82) and the median R^2 score for multi-output regression (i.e., position control) was 0.46 (ranging from 0.38 to 0.51).

B. Real-Time Control Performance Benchmarks

Performance results for the real-time control experiment are presented in Fig. 5. For each participant, performance scores from all trials are aggregated and summarized using box and violin plots. Statistical analyses were performed independently for each participant (Section II-K). All participants achieved significantly higher performance with action than position control (P1, $MD = 20.14$, $p < 10^{-2}$; P2R, $MD = 52.63$, $p < 10^{-13}$; P2L, $MD = 47.23$, $p < 10^{-10}$; P3, $MD = 62.32$, $p < 10^{-13}$; MD denotes median difference between the two control schemes). For participant P2, who took part in two experimental sessions, one with each side, there were no significant differences in performance when using the right and left sides (action control, $p = 0.39$, $MD = 2.90$; position control, $p = 0.29$, $MD = -2.50$).

A representative trial, performed with each of the two control schemes, is shown in Fig. 6 for one participant (P2R). The plots show target and user-controlled positions. Position trajectories are juxtaposed for the two control schemes. Target positions are also shown with horizontal black lines. The vertical grey lines indicate the start of the evaluation phase of the trial. The shown example corresponds to the "lateral" grip, for which the thumb is reposed and adducted and all other digits are fully flexed. It can be observed from this example that action control results in faster target reach, as well as more accurate and stable control. Two video recordings from the same experimental session are provided as supplementary material. They correspond to the last block of trials for each of the two control schemes for the same participant.

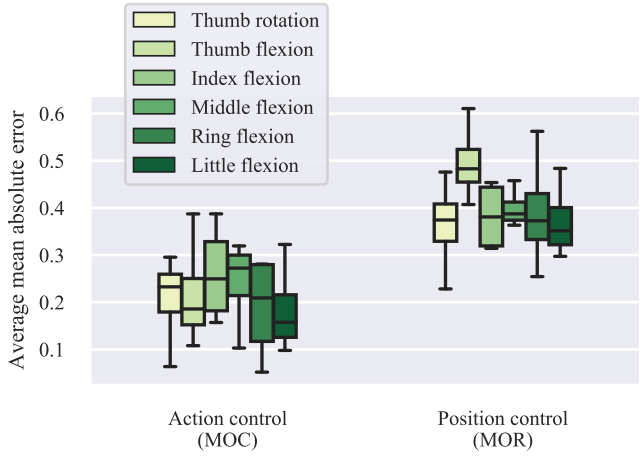

Fig. 7. Single-DOF performance comparison. Average mean absolute errors are summarized for action and position control for individual DOFs. Lower scores indicate better performance. Data from all trials are aggregated for each participant. Box plots show distribution of participant-average data ($n = 4$).

Figure 7 shows DOF-wise, participant-average mean absolute error for the two control schemes. Averages were

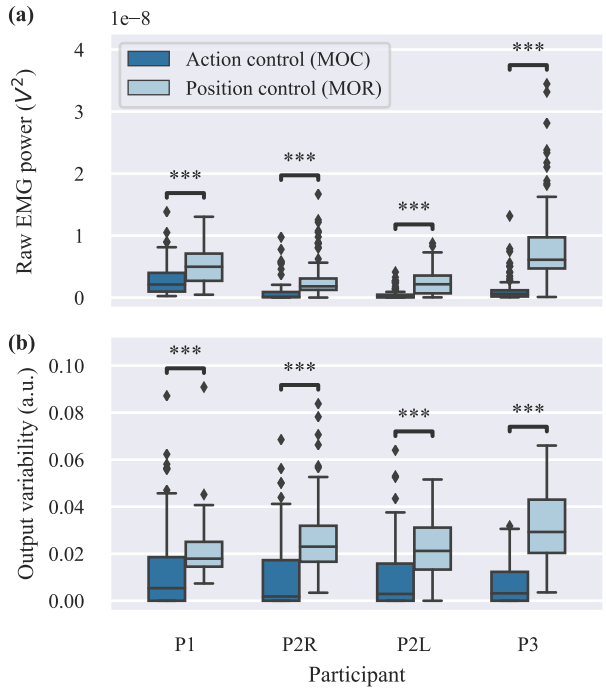

Fig. 8. Muscle contraction level and output stability comparison. (a) Average raw EMG power for all electrodes during whole trial duration. (b) Average output variability during evaluation phase. For each participant, data from all trials are aggregated ($n = 100$ in each box plot). Diamonds indicate outliers.

calculated by combining trials from all blocks and targets. For both controllers, the lowest average error was observed for the little digit DOF. The highest average errors were observed for the middle digit and the thumb for action and position control, respectively. For all DOFs, median average errors were lower with action than position control. Statistical tests were not performed due to small sample size (i.e., $n = 4$).

We now turn our attention to non-task-related measures. Firstly, we assess muscle contraction intensity levels for the two control schemes. Figure 8(a) shows average raw EMG power across all channels during the whole trial duration. For all participants, action control resulted in significantly lower average raw EMG power (P1, $PMD = 57.6\%$, $p < 10^{-10}$; P2R, $PMD = 93.1\%$, $p < 10^{-15}$; P2L, $PMD = 95.0\%$, $p < 10^{-15}$; P3, $PMD = 90.2\%$, $p < 10^{-15}$; PMD denotes percent median decrease with respect to position control values). In addition, we consider output stability by computing the average output variability (i.e., standard deviation) during the trial evaluation phase. We observed significantly lower output variability with action control for all participants (P1, $PMD = 70.0\%$, $p < 10^{-3}$; P2R, $PMD = 92.1\%$, $p < 10^{-9}$; P2L, $PMD = 86.3\%$, $p < 10^{-8}$; P3, $PMD = 89.2\%$, $p < 10^{-15}$).

C. Post-Experimental Questionnaire

The outcomes of the post-experimental questionnaire are presented in Fig. 9. All participants rated action control higher than position control in all three questions. Finally, all three participants reported an overall preference for action control.

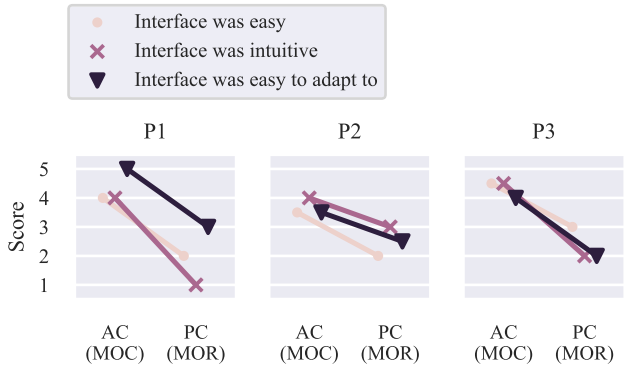

Fig. 9. Post-experimental questionnaire. Participants were asked to rate the two control schemes (i.e., action and position control) with three questions. Ratings ranged from 1 (strongly disagree) to 5 (strongly agree). Participant 2 answered the questionnaire twice, once after each session (i.e., right and left sides), and respective scores were averaged. AC, action control; PC, position control.

IV. Discussion

A. Action Control for Prosthetic Digits

We have evaluated *action control*, a novel paradigm for EMG-based prosthesis digit control based on multi-output classification. We have previously shown that this type of controller can result in comparable performance to direct joint position control in a robotic hand tele-operation task [22]. Here, we have implemented the decoder and control algorithm in real-time using surface EMG measurements and tested it with three transradial amputee participants in a total of four experimental sessions. We have shown that action control can outperform multi-output regression-based digit control in a static posture matching task. The observed improvement in performance has been both substantial and systematic across participants. Moreover, it has been systematic across evaluation measures, including both task- and non-task-related metrics. In addition, all participants rated the action control scheme higher than position control in a series of qualitative metrics and reported an overall preference for the former.

B. Relation to Previous Work

The concept of controlling actions with discrete commands (i.e., “open”, “close”, and “rest”) has been previously used for 1-DOF or 2-DOF prosthetic systems, such as wrist rotation, whole hand opening/closing, or a combination of the two [33]–[37]. In contrast, for prosthetic digit control, the focus has been on using multi-output regression to decode joint angles (i.e., positions) [9]–[12], [14], [15], [21], velocities [16] or fingertip forces [18]–[20]. Action control can be seen as an extreme, discretized case of velocity control (see Fig. 2), whereby the velocity can be either zero or take a constant value, which is only parametrized by its direction. Although we kept the velocity of the output DOFs fixed in this study, this needs not be restrictive; as is currently common in commercial prostheses, it could also be adjusted to be proportional to the overall muscle activity of the user at a given time.

In the past, a few classification-based methods have been proposed for prosthetic digit control, but with some fundamental differences when compared to our approach.

Tenore *et al.* [38] used a 12-class classifier to predict individual digit flexion/extension. By using a single-output, multi-class decoder, this approach can only be used sequentially, that is, a single DOF can be active at a time. Moreover, the absence of a "stall" class limits the controllable DOFs to be either fully open or fully closed. In comparison, our approach allows arbitrary hand configurations, including those not present in the training set, via appropriate sequences of open/close and stall commands. To achieve the control flexibility of our method, that is, simultaneous, independent control of six DOFs, with the more conventional paradigm of single-output, multi-class classification, the total number of classes should equal $6^3 = 216$. Arguably, with such an approach it would be highly impractical to collect training data and, furthermore, the accuracy of the system would likely be extremely low due to the large number of classes.

Olsson *et al.* [39] proposed a strategy that is conceptually similar to ours, however with the following three differences/limitations: 1) it is based on position rather than action control; 2) there are only two classes for each digit, fully open or close, and hence, intermediate digit positions are not feasible; 3) the study of Olsson *et al.* was limited to offline analysis, and thus, was open-loop. In comparison, the focus of our work has been on real-time control with the user in the loop. More recently, the same group proposed a neural network-based approach for real-time estimation of continuous output variables from discrete training labels, which in this case included the "stall" class. However, the experimental setup only involved two DOFs, that is, flexion/extension of the wrist and of all digits together [40]. Finally, Lukyanenko1 *et al.* [41] recently proposed a linear interpolation method for reconstructing velocities of four DOFs in a continuous space by using discrete training labels.

C. The Importance of Feedback

It is known and well accepted that interaction with a myoelectric interface that provides the user with some sort of feedback information (e.g., visual), leads to user adaptation over time. When machine learning-based controllers are deployed, this is usually manifested as an increase in task performance [42]–[44], regardless of the level of intuitiveness of the interface [14]. In fact, there exists a stream of research especially exploiting the high level of plasticity of the human brain to develop myoelectric interfaces that, despite being non-intuitive from a physiological perspective, can be mastered by the user with experience (i.e., *user learning* approach). These are typically not based on machine learning and rather rely on the user's ability to integrate feedback information to implicitly develop an inverse map of the interface so as to maximize performance at a given task [25], [45]–[50].

The role of continuous feedback in action control is of particular importance. To achieve the desired digit positions, the user has to estimate the error between the current and target positions and take the appropriate action(s) to minimize it. In other words, the algorithm on its own can be seen as an open-loop control paradigm, in which the user closes the loop by continuously integrating the available feedback information. This requirement might at first seem as a disadvantage in comparison with digit position control. One should keep in mind, however, that regression-based position control also relies heavily on the provision of continuous feedback information. This is due to biomechanical differences between a natural and an artificial limb, including, for example, a different number of controllable DOFs, a different arrangement of the available DOFs, and so on. Even in the hypothetical scenario of a perfect digit position decoder, feedback information is still useful, given that the prosthesis biomechanics are different to those of a natural limb that the user might be accustomed to. Taking into consideration the potential variance not accounted for by a digit position decoder that uses surface EMG as input signal, and prediction inaccuracies due to measurement noise and other confounding factors [51], it becomes evident that feedback plays a vital role for digit position control, despite that this approach is regarded as bio-mimetic [14]. Note that in our experiments the feedback was visual, but it could also take other invasive [52] or non-invasive [53] forms. Yet, it is not clear whether the use of alternative feedback modalities, such as electrical stimulation, can scale and/or provide functional benefit when dealing with multi-dimensional outputs—in our case, six-dimensional. This aspect warrants further investigation during real-time prosthesis use.

D. Relationship Between Velocity Control and Signal-Dependent Noise

In addition to an increase in task performance (Fig. 5), action control resulted in significantly lower muscle contraction intensity (Fig. 8(a)) and improved output stability (Fig. 8(b)). Note that participants were not given specific instructions on whether to retain or relax their muscle activity during the evaluation phase of the trials. The decrease in EMG amplitude may be attributed to the velocity control nature of the algorithm; an equal amount of muscle activation is required to open/close a digit, regardless of its current position. In stark contrast, with position control, the amount of required muscle activation is proportional to the target position; extreme digit positions require more effort from the user. Lower muscle contraction intensity translates into more effortless control for the user on the one hand, as well as less EMG signal noise on the other, which is known to be signal-dependent [54].

The improvement in control stability is likely due to the discrete nature of the output variable in the case of classification. It is well known that the EMG signal is intrinsically stochastic [55]. In the case of regression, the input noise is propagated through to the output resulting in an unstable controller and unintended prosthesis activations (i.e., jitter effect). To address this issue, it is common to post-process predictions using a low-pass filter (i.e., smoothing) [10], [14], [21]. A large amount of smoothing is typically required to achieve a satisfactory outcome, at the expense of a decrease in the responsiveness of the system. In our implementation, we set this parameter according to our previous work [14] and did not experiment thoroughly with the trade-off between stability and sensitivity. It is likely that setting the smoothing parameter to a larger value would have resulted in more

stable control, nonetheless at the cost of increasing the observable output delay. In comparison, a classifier-based controller addresses this limitation to a large extent by producing discrete output values. This type of thresholding mechanism can be viewed as an extreme case of low-pass filtering, however it avoids the large response delay associated with moving average filtering of continuous control outputs. The use of a confidence-based rejection strategy further decreases the likelihood of unintended activations [26], hence resulting in more robust and stable digit control. Finally, the increased output stability may lead to further decrease in EMG power, via reducing the amount of needed compensatory contractions.

E. Implications for Bilateral Amputation

To train regression-based systems, users are typically instructed to perform bilateral mirrored movements, whilst hand kinematic data are recorded from the contralateral to the EMG side using data gloves [9], [10], [14], [16] or motion tracking systems [11]. This approach has two main limitations: 1) from a clinical perspective, it is highly non-practical; and 2) it can only be applied in the case of unilateral amputation. Indeed, two out of three participants in our study were bilateral amputees. To address this issue, we used computer-generated prompts in combination with linear interpolation to produce regression ground truth labels (Section II-F) [21]. However, this approach can introduce label noise, given that it is not guaranteed that participants precisely track the demonstrated digit positions on the prosthesis with their phantom limb. Our position control implementation was based on our previous work, which has achieved state-of-the-art performance [14]. However, the offline decoding accuracy in the current study was lower (median R^2 0.46 vs 0.60 for the two amputee participants in [14]). This reduction in performance can be attributed to the use of different ground truth collection schemes, but this aspect warrants further investigation, for example, by directly comparing the performance of the two methods in the regression setting. In comparison, the use of classification methods avoids this pitfall since labels are discrete and constant within a trial. In other words, as long as the participant tracks the movement direction, the discrete training labels will be correct, regardless of whether they perfectly track the digit position. The feasibility of collecting noise-free ground truth labels without a requirement for bilateral mirrored training is an additional advantage of the action control approach. This feature has enabled us to recruit both unilateral and bilateral amputee participants in our experiments. To our knowledge, this is the first demonstration of real-time, multi-DOF myoelectric digit control in bilateral upper-limb amputees.

It is worth noting that despite having demonstrated here the feasibility of individual digit control in bilateral amputees, in our experiments participants controlled digits corresponding to a single side at a time. Extending our approach to both sides would be trivial from an algorithmic perspective, as it would only require using two identical EMG processing and digit control pipelines. Nevertheless, from a user's perspective, it might prove challenging considering the high dimensionality of the control space (i.e., 12 DOFs).

F. Limitations

Our study has a few limitations. Participants controlled a computer interface rather than an actual prosthesis. This was due to the lack of position encoders on the prosthesis that we used in our experiments, which were required for benchmarking our proposed algorithm against the regression-based approach. Moreover, our real-time control task only involved digit closing actions; intermediate finger postures and opening motions were not included. This design choice was due to a number of practical reasons: 1) the lack of position encoders hindered the demonstration of intermediate digit postures on the prosthesis; and 2) digit opening motions were not included as it would not be straightforward to test them in the case of position control. In order to evaluate a digit opening motion, participants would be required to start the trial from a closed state, which corresponds to non-zero muscle activity. For action control, it would have been trivial to test digit opening motions, as given the velocity control nature of the algorithm, it is feasible to assume a closed initial position without any corresponding muscle activity. However, the aim of the study was to compare the performance of the two control schemes and, hence, we decided to exclude digit opening motions. Our decision was further dictated by a requirement to keep the total experiment time within reasonable limits to avoid muscle and mental fatigue. Given this trade-off, we opted for digit closing and grasping postures only, which are particularly relevant in prosthetics from a functional perspective.

Although the capability of the action controller to produce arbitrary postures was not explicitly demonstrated, such postures are indeed feasible, despite the discrete nature of the decoder. The capability to achieve intermediate postures is directly related to the ability of the decoder to correctly predict the "stall" class. In offline analysis, we have previously observed that this class can be recognized with very high sensitivity (median recall of 0.91, as compared to 0.56 and 0.50 for the "open" and "close" classes, respectively) [23]. Moreover, many target postures comprised single-digit closing motions. Considering that our performance score computes the average error across all six outputs, unintended activations of the non-moving DOFs would result in poor performance scores. In other words, the ability of the algorithm to correctly predict the "stall" class was implicitly taken into account by our performance metric and choice of testing postures. Finally, given the comparable recall (i.e., sensitivity) between the "open" and "close" classes in offline analysis [23], we do not expect a substantial difference in real-time performance between the two classes.

Another limitation of the study is that it involved only matching static postures. This could have potentially biased measured performance towards the action control paradigm. This is due to the observation that, once a target posture has been achieved, the user can hold it without exerting any muscle activity. Whether this feature is beneficial for real-life prosthetic use remains to be investigated during real-time operation of a prosthesis mounted on a socket.

Taking everything into consideration, further validation of our proposed algorithm is required, either using standardised

pre-clinical tests, such as the target achievement control (TAC) test [56], or ideally during control of a real prosthesis. In the future, we will transfer the control interface from the computer display onto a prosthesis and evaluate performance during activities of daily living, such as object grasping. This will further allow us to assess the performance of the algorithm for intermediate digit positions and opening motions, as well as evaluate its robustness under dynamic limb position and prosthesis load conditions. Ideally, our controller should be tested with a larger number of participants to further validate the results of this study.

V. Conclusion

We have proposed and evaluated a novel control scheme for myoelectric digit control with transradial amputee participants. Our proposed algorithm, termed *action control*, is based on multi-output, multi-class classification and relies on the provision of continuous visual feedback to the user. We have shown that it can significantly outperform the state-of-the art regression-based approach with respect to several task- and non-task-related measures. In the future, we will further evaluate the performance of the method under real-life scenarios by transferring the task space from a computer interface onto a prosthesis.

Acknowledgment

The authors are thankful to the three amputee volunteers for their participation in the study and to Sigrid Dupan for providing feedback on an earlier version of the manuscript.

References

[1] D. Farina *et al.*, "The extraction of neural information from the surface EMG for the control of upper-limb prostheses: Emerging avenues and challenges," *IEEE Trans. Neural Syst. Rehabil. Eng.*, vol. 22, no. 4, pp. 797–809, Jul. 2014.

[2] G. P. Kontoudis, M. V. Liarokapis, A. G. Zisimatos, C. I. Mavrogiannis, and K. J. Kyriakopoulos, "Open-source, anthropomorphic, underactuated robot hands with a selectively lockable differential mechanism: Towards affordable prostheses," in *Proc. IEEE/RSJ Int. Conf. Intell. Robots Syst. (IROS)*, Sep. 2015, pp. 5857–5862.

[3] A. Fougner, Ø. Stavdahl, P. J. Kyberd, Y. G. Losier, and P. A. Parker, "Control of upper limb prostheses: Terminology and proportional myoelectric control—A review," *IEEE Trans. Neural Syst. Rehabil. Eng.*, vol. 20, no. 5, pp. 663–677, Sep. 2012.

[4] S. Muceli, N. Jiang, and D. Farina, "Extracting signals robust to electrode number and shift for online simultaneous and proportional myoelectric control by factorization algorithms," *IEEE Trans. Neural Syst. Rehabil. Eng.*, vol. 22, no. 3, pp. 623–633, May 2014.

[5] J. M. Hahne *et al.*, "Linear and nonlinear regression techniques for simultaneous and proportional myoelectric control," *IEEE Trans. Neural Syst. Rehabil. Eng.*, vol. 22, no. 2, pp. 269–279, Mar. 2014.

[6] L. H. Smith, T. A. Kuiken, and L. J. Hargrove, "Real-time simultaneous and proportional myoelectric control using intramuscular EMG," *J. Neural Eng.*, vol. 11, no. 6, Dec. 2014.

[7] N. Jiang, I. Vujaklija, H. Rehbaum, B. Graimann, and D. Farina, "Is accurate mapping of EMG signals on kinematics needed for precise online myoelectric control?" *IEEE Trans. Neural Syst. Rehabil. Eng.*, vol. 22, no. 3, pp. 549–558, May 2014.

[8] J. M. Hahne, M. A. Schweisfurth, M. Koppe, and D. Farina, "Simultaneous control of multiple functions of bionic hand prostheses: Performance and robustness in end users," *Sci. Robot.*, vol. 3, no. 19, Jun. 2018.

[9] R. J. Smith, F. Tenore, D. Huberdeau, R. Etienne-Cummings, and N. V. Thakor, "Continuous decoding of finger position from surface EMG signals for the control of powered prostheses," in *Proc. 30th Annu. Int. Conf. IEEE Eng. Med. Biol. Soc.*, Aug. 2008, pp. 197–200.

[10] C. Cipriani *et al.*, "Online myoelectric control of a dexterous hand prosthesis by transradial amputees," *IEEE Trans. Neural Syst. Rehabil. Eng.*, vol. 19, no. 3, pp. 260–270, Jun. 2011.

[11] J. G. Ngeo, T. Tamei, and T. Shibata, "Continuous and simultaneous estimation of finger kinematics using inputs from an EMG-to-muscle activation model," *J. Neuroeng. Rehabil.*, vol. 11, no. 1, p. 122, 2014.

[12] A. Krasoulis, S. Vijayakumar, and K. Nazarpour, "Evaluation of regression methods for the continuous decoding of finger movement from surface EMG and accelerometry," in *Proc. 7th Int. IEEE/EMBS Conf. Neural Eng. (NER)*, Apr. 2015, pp. 631–634.

[13] A. Krasoulis, K. Nazarpour, and S. Vijayakumar, "Towards low-dimensionsal proportional myoelectric control," in *Proc. 37th Annu. Int. Conf. IEEE Eng. Med. Biol. Soc. (EMBC)*, Aug. 2015, pp. 7155–7158.

[14] A. Krasoulis, S. Vijayakumar, and K. Nazarpour, "Effect of user practice on prosthetic finger control with an intuitive myoelectric decoder," *Frontiers Neurosci.*, vol. 13, Sep. 2019.

[15] W. Guo *et al.*, "Long exposure convolutional memory network for accurate estimation of finger kinematics from surface electromyographic signals," *J. Neural Eng.*, vol. 18, no. 2, Apr. 2021.

[16] M. Xiloyannis, C. Gavriel, A. A. C. Thomik, and A. A. Faisal, "Gaussian process autoregression for simultaneous proportional multi-modal prosthetic control with natural hand kinematics," *IEEE Trans. Neural Syst. Rehabil. Eng.*, vol. 25, no. 10, pp. 1785–1801, Oct. 2017.

[17] C. Castellini, E. Gruppioni, A. Davalli, and G. Sandini, "Fine detection of grasp force and posture by amputees via surface electromyography," *J. Physiol. Paris*, vol. 103, nos. 3–5, pp. 255–262, May/Sep. 2009.

[18] A. Gijsberts *et al.*, "Stable myoelectric control of a hand prosthesis using non-linear incremental learning," *Frontiers Neurorobot.*, vol. 8, p. 8, Feb. 2014.

[19] A. Gailey, P. Artemiadis, and M. Santello, "Proof of concept of an online EMG-based decoding of hand postures and individual digit forces for prosthetic hand control," *Frontiers Neurol.*, vol. 8, p. 7, Feb. 2017.

[20] M. Barsotti, S. Dupan, I. Vujaklija, S. Dosen, A. Frisoli, and D. Farina, "Online finger control using high-density EMG and minimal training data for robotic applications," *IEEE Robot. Autom. Lett.*, vol. 4, no. 2, pp. 217–223, Apr. 2019.

[21] K. Z. Zhuang *et al.*, "Shared human–robot proportional control of a dexterous myoelectric prosthesis," *Nature Mach. Intell.*, vol. 1, no. 9, pp. 400–411, Sep. 2019.

[22] A. Krasoulis, S. Vijayakumar, and K. Nazarpour, "Continuous versus discrete simultaneous control of prosthetic fingers," in *Proc. 40th Annu. Int. Conf. IEEE Eng. Med. Biol. Soc. (EMBC)*, Jul. 2018, pp. 3774–3777.

[23] A. Krasoulis and K. Nazarpour, "Myoelectric digit action decoding with multi-output, multi-class classification: An offline analysis," *Sci. Rep.*, vol. 10, no. 1, pp. 1–10, Dec. 2020.

[24] A. Krasoulis, I. Kyranou, M. S. Erden, K. Nazarpour, and S. Vijayakumar, "Improved prosthetic hand control with concurrent use of myoelectric and inertial measurements," *J. NeuroEng. Rehabil.*, vol. 14, no. 1, pp. 1–14, Dec. 2017.

[25] M. Dyson, J. Barnes, and K. Nazarpour, "Myoelectric control with abstract decoders," *J. Neural Eng.*, vol. 15, no. 5, Oct. 2018, Art. no. 056003.

[26] A. Krasoulis, S. Vijayakumar, and K. Nazarpour, "Multi-grip classification-based prosthesis control with two EMG-IMU sensors," *IEEE Trans. Neural Syst. Rehabil. Eng.*, vol. 28, no. 2, pp. 508–518, Feb. 2020.

[27] E. J. Scheme, B. S. Hudgins, and K. B. Englehart, "Confidence-based rejection for improved pattern recognition myoelectric control," *IEEE Trans. Biomed. Eng.*, vol. 60, no. 6, pp. 1563–1570, Jun. 2013.

[28] N. Jiang, H. Rehbaum, I. Vujaklija, B. Graimann, and D. Farina, "Intuitive, online, simultaneous, and proportional myoelectric control over two degrees-of-freedom in upper limb amputees," *IEEE Trans. Neural Syst. Rehabil. Eng.*, vol. 22, no. 3, pp. 501–510, May 2014.

[29] J. M. Hahne, M. Markovic, and D. Farina, "User adaptation in myoelectric man-machine interfaces," *Sci. Rep.*, vol. 7, no. 1, p. 4437, Dec. 2017.

[30] K. Lyons and B. Margolis, "AxoPy: A Python library for implementing human-computer interface experiments," *J. Open Source Softw.*, vol. 4, no. 34, p. 1191, Feb. 2019.

[31] F. Pedregosa *et al.*, "Scikit-learn: Machine learning in Python," *J. Mach. Learn. Res.*, vol. 12, no. 10, pp. 2825–2830, Jul. 2017.

[32] R. Vallat, "Pingouin: Statistics in Python," *J. Open Source Softw.*, vol. 3, no. 1026, p. 331, 2018.

[33] A. J. Young, L. H. Smith, E. J. Rouse, and L. J. Hargrove, "Classification of simultaneous movements using surface EMG pattern recognition," *IEEE Trans. Biomed. Eng.*, vol. 60, no. 5, pp. 1250–1258, May 2013.

[34] A. J. Young, L. H. Smith, E. J. Rouse, and L. J. Hargrove, "A comparison of the real-time controllability of pattern recognition to conventional myoelectric control for discrete and simultaneous movements," *J. NeuroEng. Rehabil.*, vol. 11, no. 1, p. 5, 2014.

[35] S. M. Wurth and L. J. Hargrove, "A real-time comparison between direct control, sequential pattern recognition control and simultaneous pattern recognition control using a Fitts' law style assessment procedure," *J. NeuroEng. Rehabil.*, vol. 11, no. 1, p. 91, 2014.
[36] M. Ortiz-Catalan, B. Håkansson, and R. Brånemark, "Real-time and simultaneous control of artificial limbs based on pattern recognition algorithms," *IEEE Trans. Neural Syst. Rehabil. Eng.*, vol. 22, no. 4, pp. 756–764, Jul. 2014.
[37] M. Ortiz-Catalan, F. Rouhani, R. Brånemark, and B. Hakansson, "Offline accuracy: A potentially misleading metric in myoelectric pattern recognition for prosthetic control," in *Proc. 37th Annu. Int. Conf. IEEE Eng. Med. Biol. Soc. (EMBC)*, Aug. 2015, pp. 1140–1143.
[38] F. V. G. Tenore, A. Ramos, A. Fahmy, S. Acharya, R. Etienne-Cummings, and N. V. Thakor, "Decoding of individuated finger movements using surface electromyography," *IEEE Trans. Biomed. Eng.*, vol. 56, no. 5, pp. 1427–1434, May 2009.
[39] A. E. Olsson, P. Sager, E. Andersson, A. Björkman, N. Malešević, and C. Antfolk, "Extraction of multi-labelled movement information from the raw HD-sEMG image with time-domain depth," *Sci. Rep.*, vol. 9, no. 1, pp. 1–10, Dec. 2019.
[40] A. E. Olsson, N. Malešević, A. Björkman, and C. Antfolk, "Learning regularized representations of categorically labelled surface EMG enables simultaneous and proportional myoelectric control," *J. NeuroEng. Rehabil.*, vol. 18, no. 1, pp. 1–19, Dec. 2021.
[41] P. Lukyanenko, H. A. Dewald, J. Lambrecht, R. F. Kirsch, D. J. Tyler, and M. R. Williams, "Stable, simultaneous and proportional 4-DoF prosthetic hand control via synergy-inspired linear interpolation: A case series," *J. NeuroEng. Rehabil.*, vol. 18, no. 1, pp. 1–15, Dec. 2021.
[42] N. E. Bunderson and T. A. Kuiken, "Quantification of feature space changes with experience during electromyogram pattern recognition control," *IEEE Trans. Neural Syst. Rehabil. Eng.*, vol. 20, no. 3, pp. 239–246, May 2012.
[43] M. Powell, R. Kaliki, and N. Thakor, "User training for pattern recognition-based myoelectric prostheses: Improving phantom limb movement consistency and distinguishability," *IEEE Trans. Neural Syst. Rehabil. Eng.*, vol. 22, no. 3, pp. 522–532, May 2014.
[44] L. J. Hargrove, L. A. Miller, K. Turner, and T. A. Kuiken, "Myoelectric pattern recognition outperforms direct control for transhumeral amputees with targeted muscle reinnervation: A randomized clinical trial," *Sci. Rep.*, vol. 7, no. 1, Dec. 2017.
[45] S. M. Radhakrishnan, S. N. Baker, and A. Jackson, "Learning a novel myoelectric-controlled interface task," *J. Neurophysiol.*, vol. 100, no. 4, pp. 2397–2408, Oct. 2008.
[46] K. Nazarpour, A. Barnard, and A. Jackson, "Flexible cortical control of task-specific muscle synergies," *J. Neurosci.*, vol. 32, no. 36, pp. 12349–12360, Sep. 2012.
[47] C. W. Antuvan, M. Ison, and P. Artemiadis, "Embedded human control of robots using myoelectric interfaces," *IEEE Trans. Neural Syst. Rehabil. Eng.*, vol. 22, no. 4, pp. 820–827, Jan. 2014.
[48] M. Ison and P. Artemiadis, "Proportional myoelectric control of robots: Muscle synergy development drives performance enhancement, retainment, and generalization," *IEEE Trans. Robot.*, vol. 31, no. 2, pp. 259–268, Apr. 2015.
[49] M. Ison, I. Vujaklija, B. Whitsell, D. Farina, and P. Artemiadis, "High-density electromyography and motor skill learning for robust long-term control of a 7-DoF robot arm," *IEEE Trans. Neural Syst. Rehabil. Eng.*, vol. 24, no. 4, pp. 424–433, Apr. 2016.
[50] M. Markovic, M. Varel, M. A. Schweisfurth, A. F. Schilling, and S. Dosen, "Closed-loop multi-amplitude control for robust and dexterous performance of myoelectric prosthesis," *IEEE Trans. Neural Syst. Rehabil. Eng.*, vol. 28, no. 2, pp. 498–507, Feb. 2020.
[51] I. Kyranou, S. Vijayakumar, and M. S. Erden, "Causes of performance degradation in non-invasive electromyographic pattern recognition in upper limb prostheses," *Frontiers Neurorobot.*, vol. 12, pp. 1–22, Sep. 2018.
[52] E. D'Anna *et al.*, "A closed-loop hand prosthesis with simultaneous intraneural tactile and position feedback," *Sci. Robot.*, vol. 4, no. 27, Feb. 2019.
[53] B. Stephens-Fripp, G. Alici, and R. Mutlu, "A review of non-invasive sensory feedback methods for transradial prosthetic hands," *IEEE Access*, vol. 6, pp. 6878–6899, 2018.
[54] C. M. Harris and D. M. Wolpert, "Signal-dependent noise determines motor planning," *Nature*, vol. 394, no. 6695, pp. 780–784, Aug. 1998.
[55] M. B. I. Reaz, M. S. Hussain, and F. Mohd-Yasin, "Techniques of EMG signal analysis: Detection, processing, classification and applications," *Biol. Procedures*, vol. 8, no. 1, pp. 11–35, Dec. 2006.
[56] A. M. Simon, L. J. Hargrove, B. A. Lock, and T. A. Kuiken, "The target achievement control test: Evaluating real-time myoelectric pattern recognition control of a multifunctional upper-limb prosthesis," *J. Rehabil. Res. Develop.*, vol. 48, no. 6, p. 619, 2011.